Frequency-domain methods for the analysis of offshore wind turbine foundations

Karl Merz
SINTEF Energy Research

With contributions from
Lene Eliassen
NTNU/Statkraft

January 21, 2016

Additional thanks to Sebastian Schafhirt and Jason Jonkman for providing simulation results for verification.

A linear state-space model

$$\mathbf{L}\frac{d\mathbf{x}}{dt} = \mathbf{A}\mathbf{x} + \mathbf{B}\mathbf{u}$$

$$\mathbf{y} = \mathbf{C}\mathbf{x} + \mathbf{D}\mathbf{u}$$

L, A, B, C, D: sparse
$\mathbf{L}^{-1}$: full

Motto:
"If we can put it into state space then we can solve it.
If we can put it into linear state space then we can understand it."

Outline of a frequency domain calculation

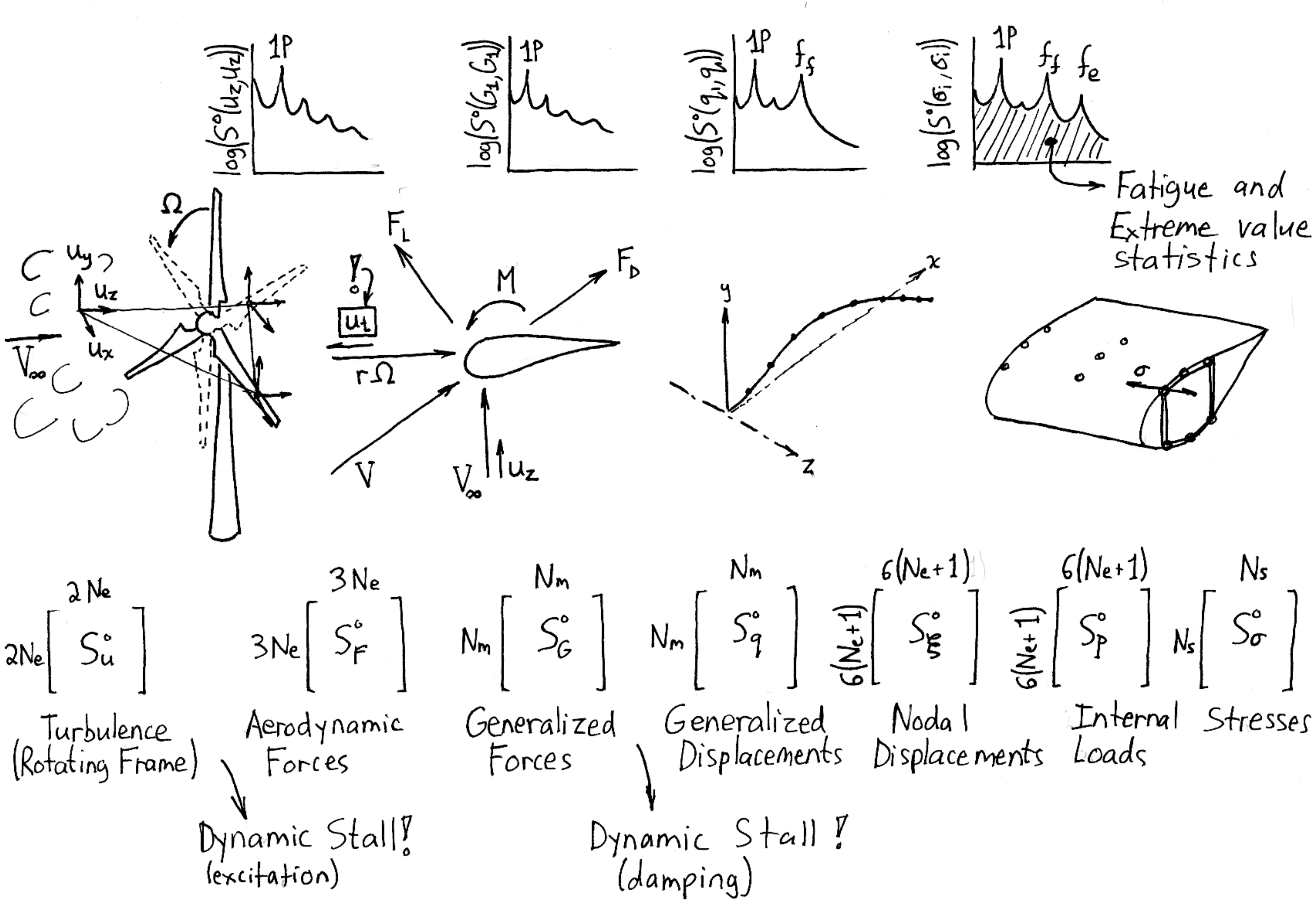

Why frequency-domain analysis?

Linear, superposition applies.

Linear time-invariant matrix equations can be partitioned, and examined piece-by-piece.

Modal frequencies and damping.

Stability properties of the system can be computed directly.

Stochastic cycle counts and estimates of extremes can be obtained without the use of random numbers.

Numerically smooth, nice for optimization.

Analysis of high-frequency dynamics is straightforward.

Speed of calculation.

Within a given load case, each frequency can be considered independently, computed in parallel.

Control gain tuning, recipes for "optimal" control.

Well-designed control systems are robust against (small) inaccuracies in modelling.

Why *not* frequency-domain analysis?

Transient load cases

Accuracy.

Hypotheses, results, designs generated using frequency-domain analysis should in the later stages be verified with nonlinear time-domain simulations.

Rotationally-sampled isotropic turbulence, axial and tangential components

$$s = \sqrt{(V_\infty \tau)^2 + r_1^2 + r_2^2 - 2 r_1 r_2 \cos \Omega\tau}$$

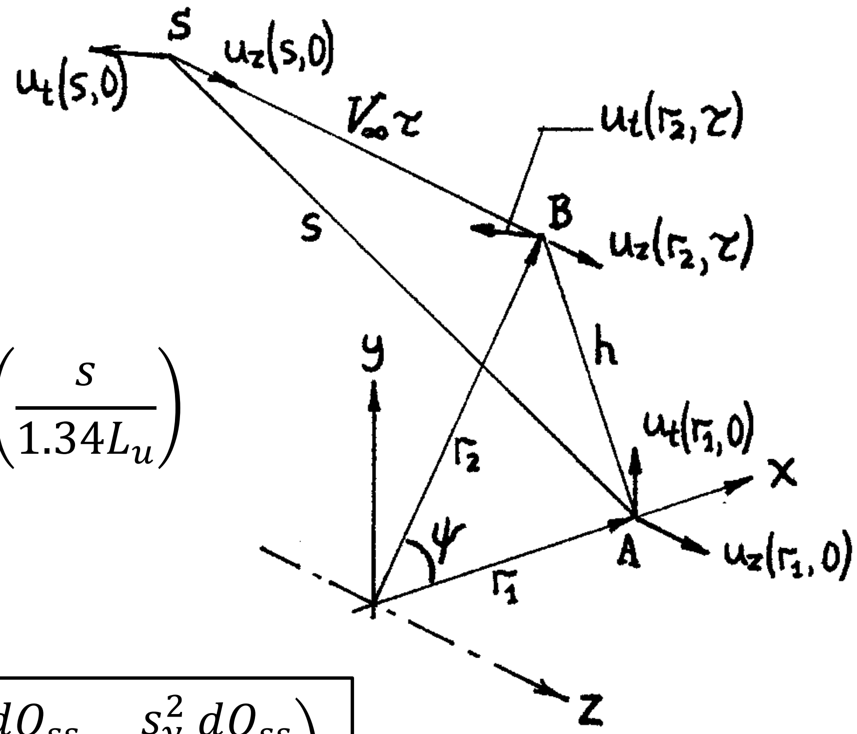

$$Q_{ss} = \frac{2\sigma_u^2}{\Gamma(1/3)} \left(\frac{s}{2.68 L_u}\right)^{1/3} K_{1/3}\left(\frac{s}{1.34 L_u}\right)$$

$$\frac{dQ_{ss}}{ds} = -\frac{2\sigma_u^2}{\Gamma(1/3)} \left(\frac{1}{1.34 L_u}\right) \left(\frac{s}{2.68 L_u}\right)^{1/3} K_{-2/3}\left(\frac{s}{1.34 L_u}\right)$$

$$Q_{zz} = Q_{ss} + \frac{s}{2}\frac{dQ_{ss}}{ds} - \frac{s_z^2}{2s}\frac{dQ_{ss}}{ds}$$

$$\boxed{Q_{tt} = (\sin \Omega\tau) \frac{s_x s_y}{2s}\frac{dQ_{ss}}{ds} + (\cos \Omega\tau)\left(Q_{ss} + \frac{s}{2}\frac{dQ_{ss}}{ds} - \frac{s_y^2}{2s}\frac{dQ_{ss}}{ds}\right)}$$

$$Q_{zt}, Q_{tz} \approx 0$$

$$Q_{ij} \equiv E\left[u_i(r_1)\, u_j(r_1 + s)\right] = E\left[u_i(r_1, t)\, u_j(r_2, t + \tau)\right]$$

Rotationally-sampled turbulence correlation functions, single blade, near tip

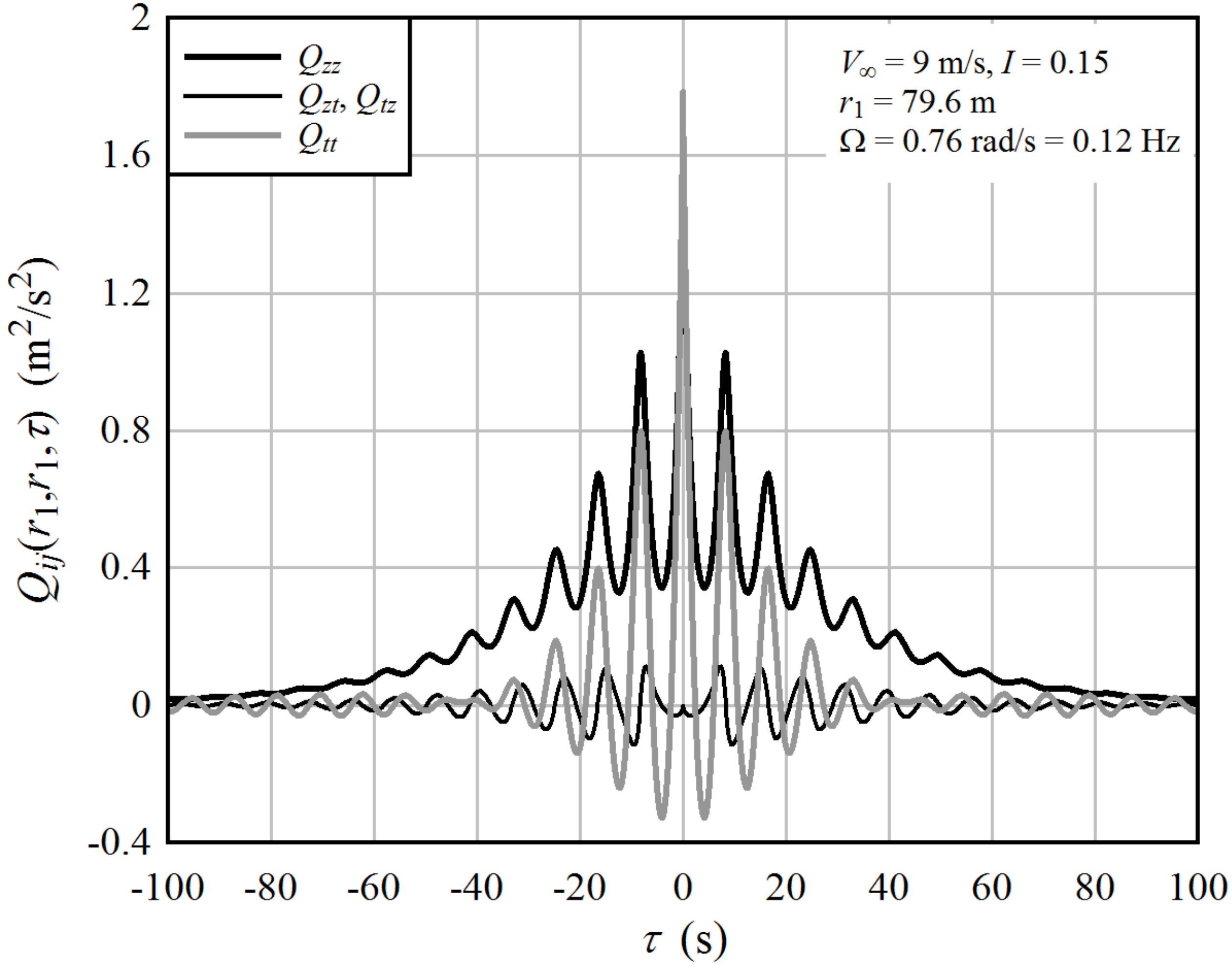

Rotationally-sampled turbulence spectrum near blade tip

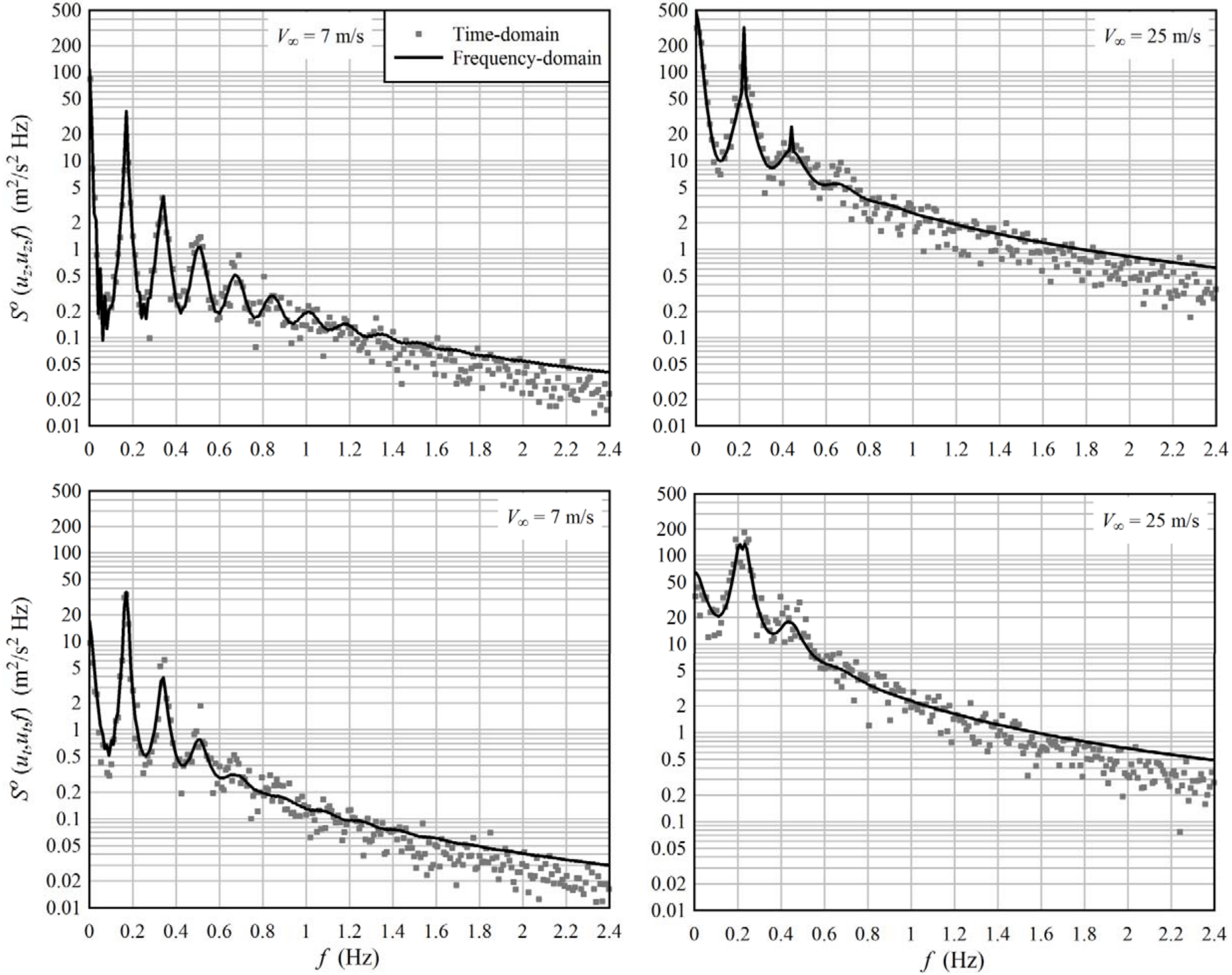

Note: not the DTU turbine. Stall-regulated blades.

Multi-blade coordinate transform of rotationally-sampled turbulence

$$\mathbf{Q}^{\psi}(r_1, r_2, \tau) = \mathbf{T}^{\psi}_{B,p}(0) \;\; \mathbf{Q}_{ij}(s_{pq}(\tau), 0) \;\; \left[\mathbf{T}^{\psi}_{B,q}(\tau)\right]^T$$

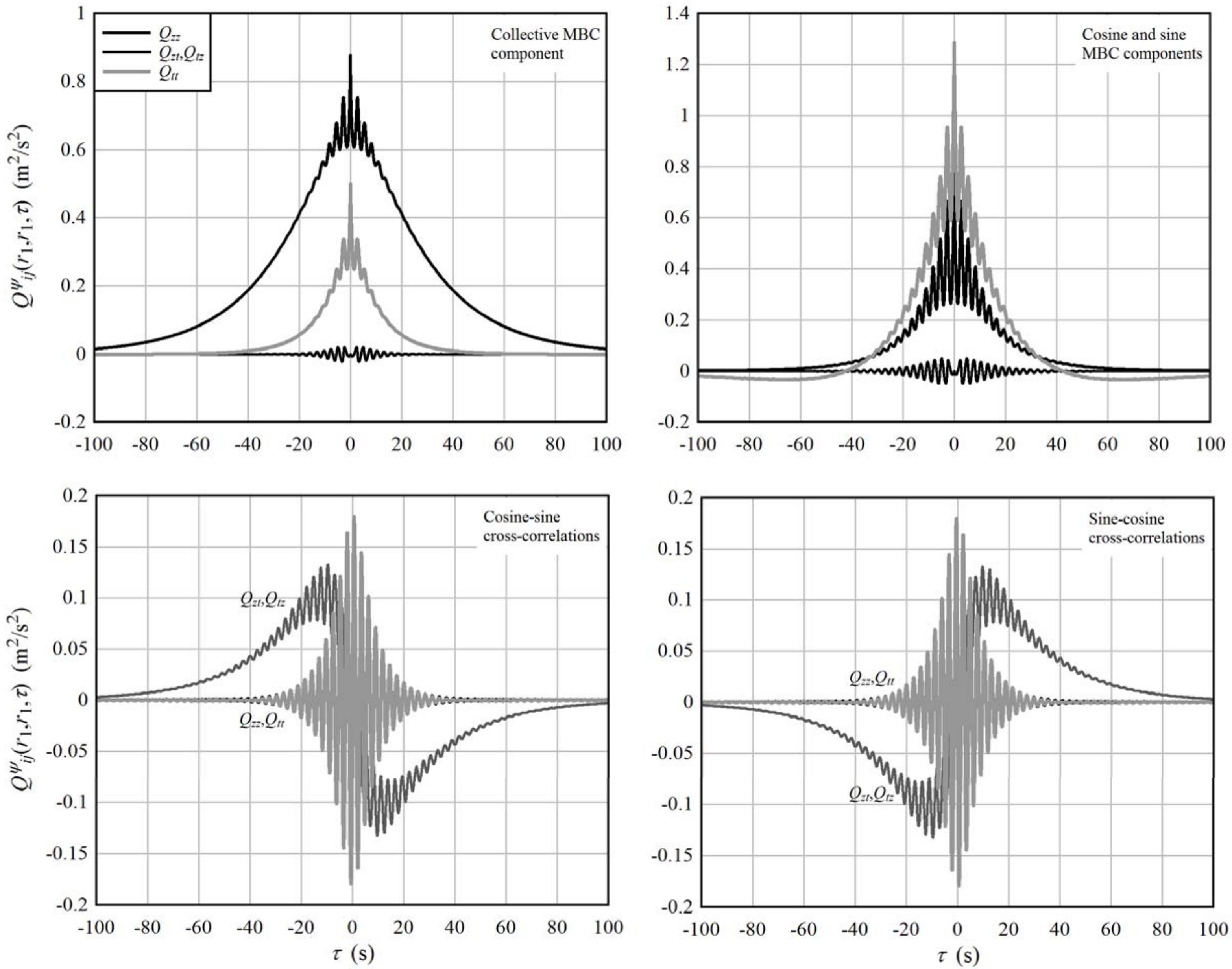

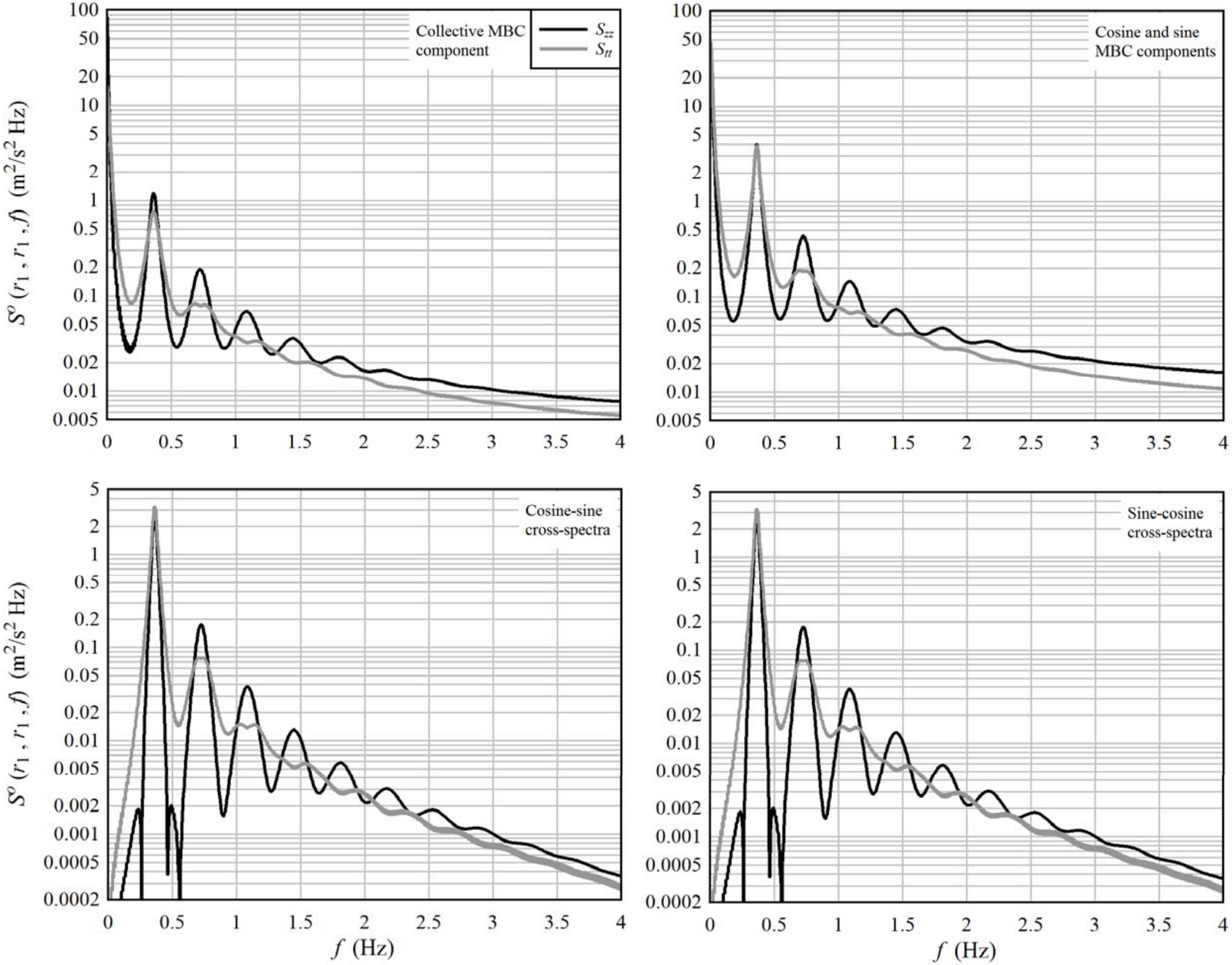
Collective MBC component
S_{zz}
S_{tt}
Cosine and sine MBC components
Cosine-sine cross-spectra
Sine-cosine cross-spectra
$S^o(r_1, r_1, f)$ (m^2/s^2 Hz)
f (Hz)

Wave loads: "MacCamy-Fuchs plus Morison drag plus Wheeler stretching"

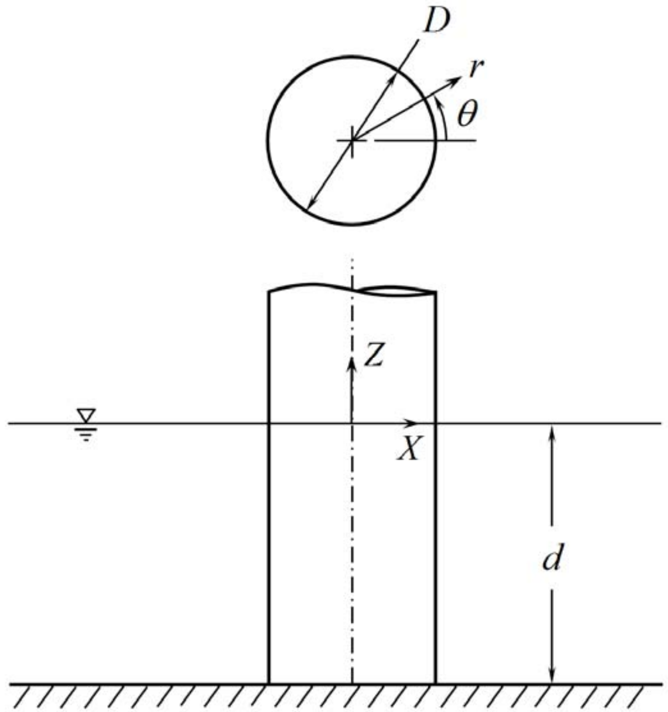

$$\Phi = \frac{g\zeta_0}{\omega}\exp(i\omega t)\frac{\cosh k_r(z+d)}{\cosh k_r d}$$

$$\times\sum_{m=0}^{\infty} i^{m+1}(-1)^m \grave{o}_m \left(J_m(k_r r) - f_m(R)\left[J_m(k_r r) - iY_m(k_r r)\right]\right)\cos m\theta,$$

$$f_m(R) := \frac{-k_r J_{m+1}(k_r R) + \dfrac{m}{R}J_m(k_r R)}{-k_r J_{m+1}(k_r R) + \dfrac{m}{R}J_m(k_r R) - i\left(-k_r Y_{m+1}(k_r R) + \dfrac{m}{R}Y_m(k_r R)\right)}$$

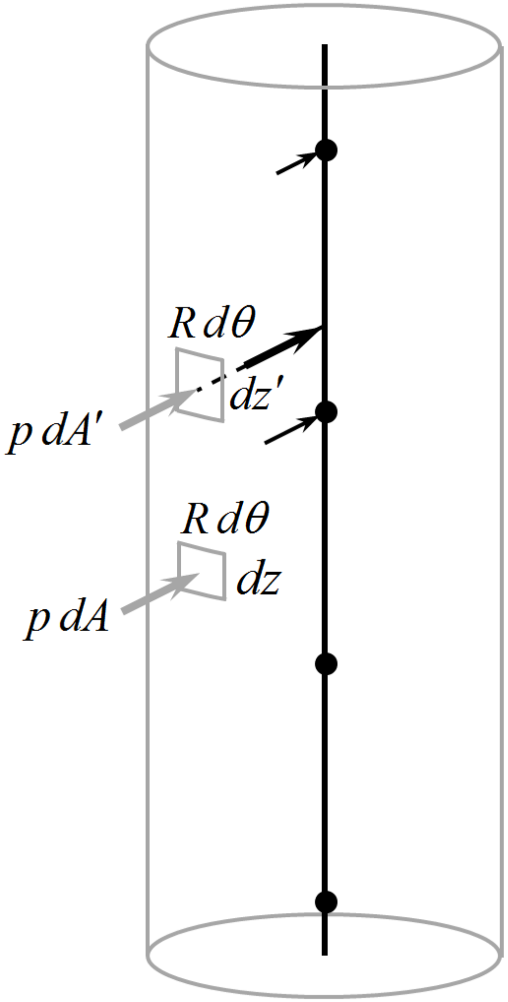

$$z + d = (z' + d)\frac{d}{d+\zeta}$$

$$dz = dz'\frac{d}{d+\zeta}$$

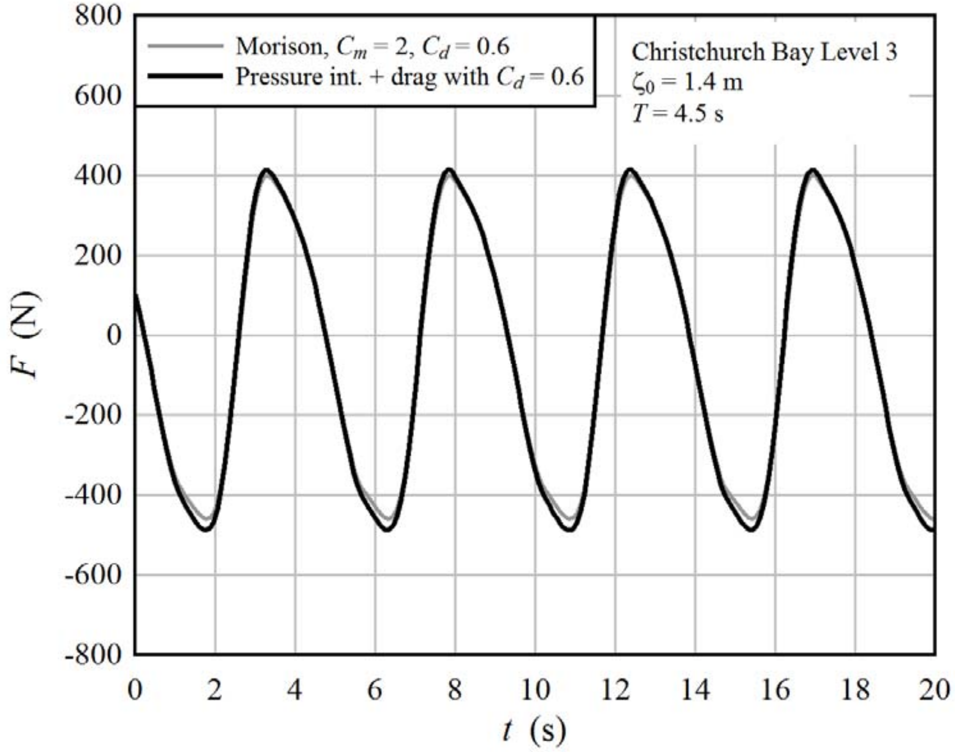

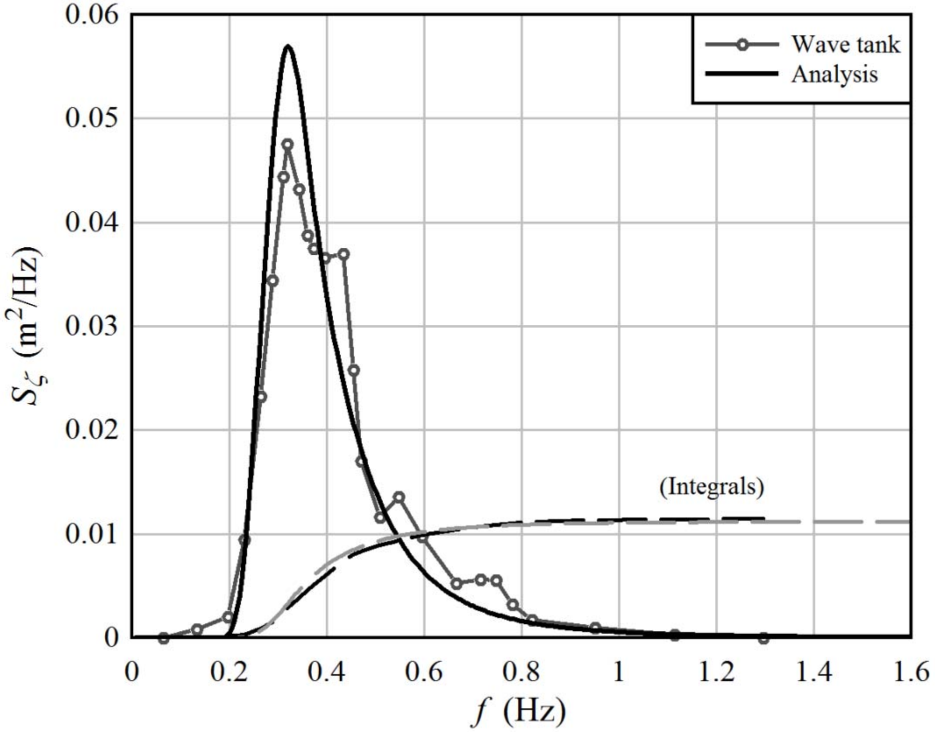

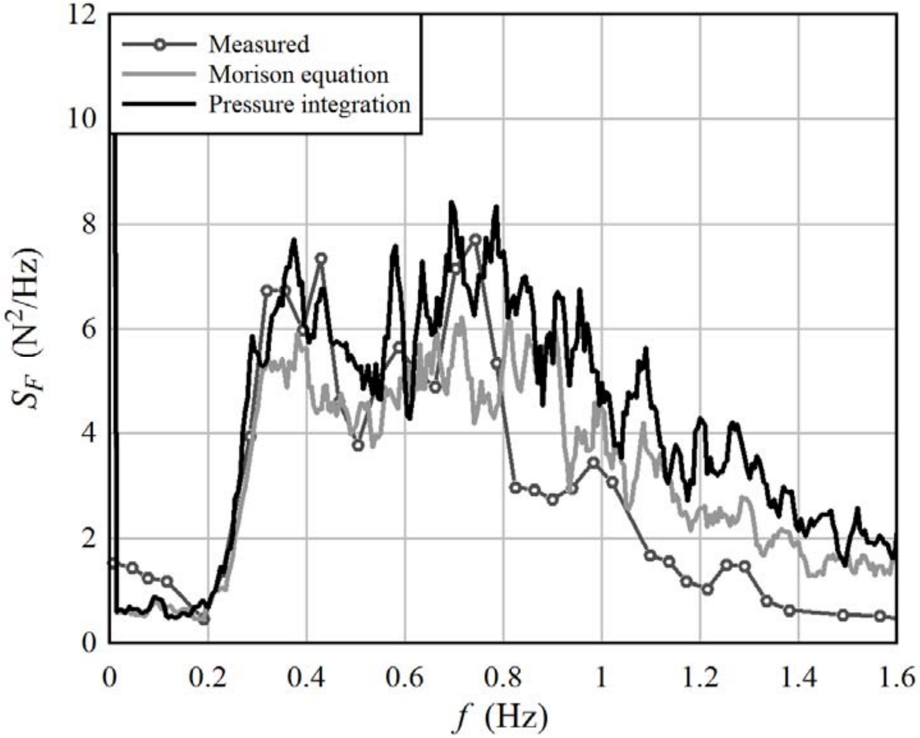

Wave tank data from: Isaacson M, Baldwin J. Measured and predicted random wave forces near the free surface. Applied Ocean Research 12 (1990) 188-199.

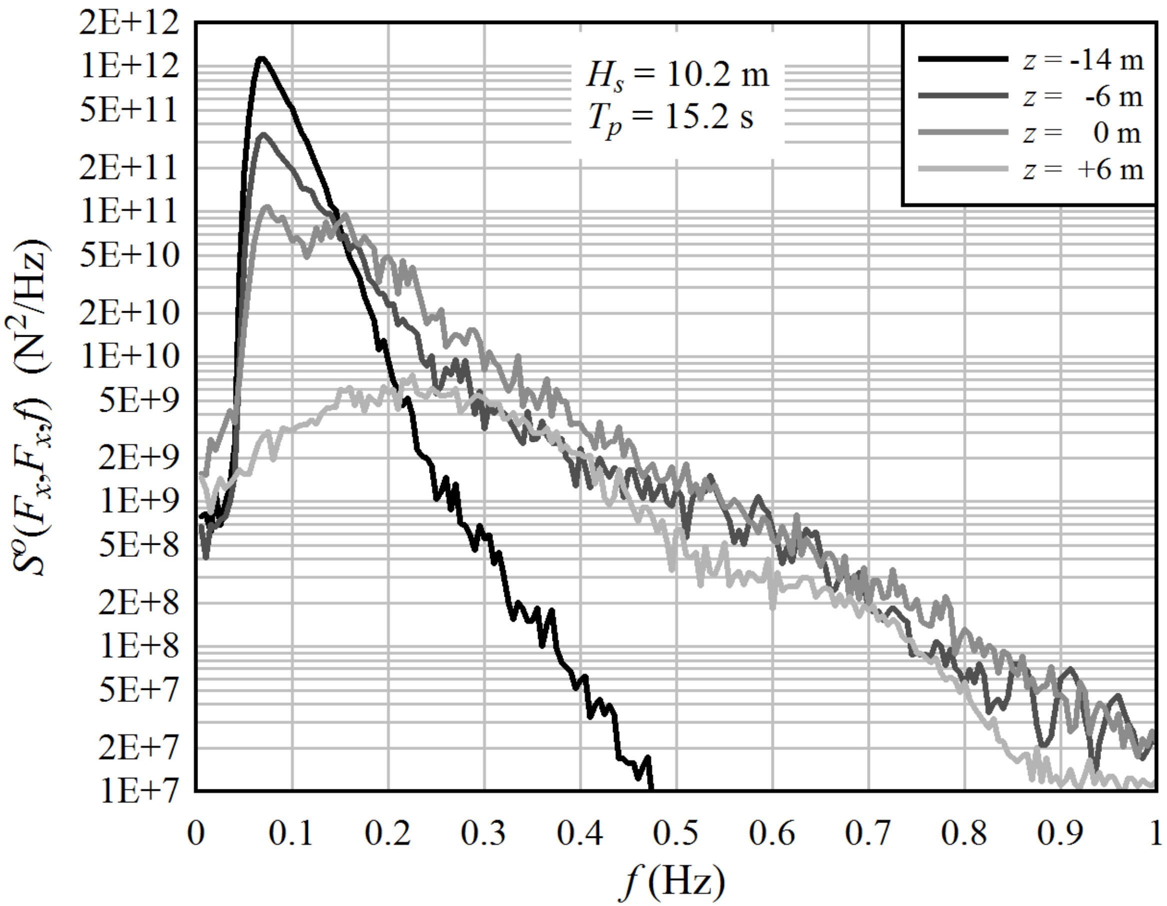

Some second-order effects are accounted for.
Not a true second-order method. Second-order frequency-domain methods are available and could be implemented.

Commercial codes can also be used to generate the input time series.

Linearized DTU Basic Wind Energy Controller

4 - 7 m/s

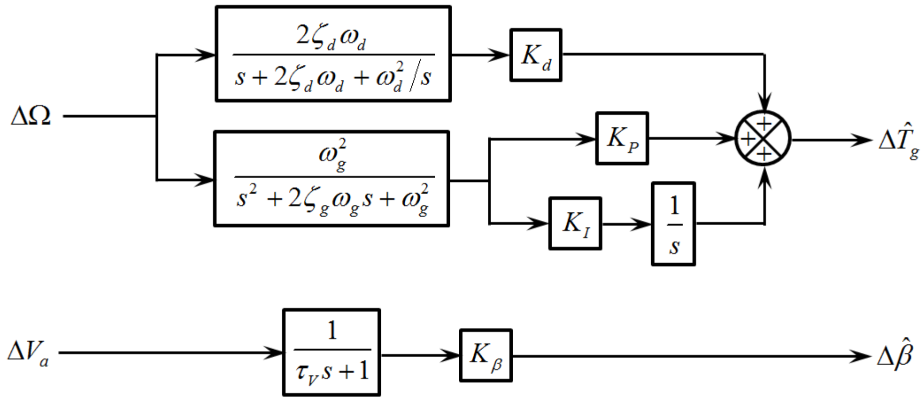

8 - 11 m/s

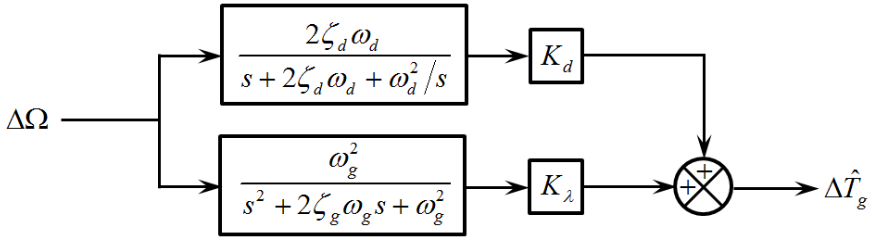

12 - 25 m/s

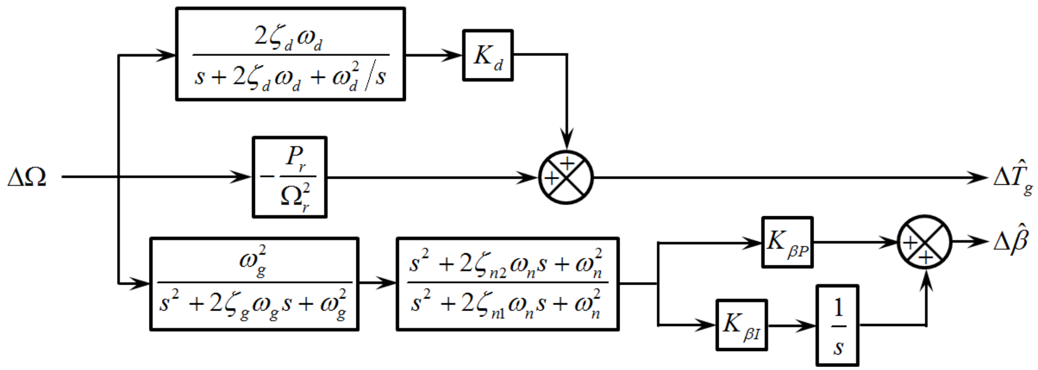

Generator model

Mean:

$$\left(\omega_0 \mathbf{T}_a^\theta \mathbf{\Lambda} \frac{d\mathbf{T}_\theta^a}{d\theta} + \mathbf{T}_a^\theta \mathbf{R} \mathbf{T}_\theta^a\right)\mathbf{i}_0^\theta = -\mathbf{v}_0^\theta - \omega_0 \mathbf{T}_a^\theta \frac{d\mathbf{T}_\theta^a}{d\theta}\boldsymbol{\lambda}_r^\theta$$

Fluctuations:

$$\mathbf{T}_a^\theta \mathbf{\Lambda} \mathbf{T}_\theta^a \frac{d\,\Delta\mathbf{i}^\theta}{dt} = -\left(\omega_0 \mathbf{T}_a^\theta \mathbf{\Lambda} \frac{d\mathbf{T}_\theta^a}{d\theta} + \mathbf{T}_a^\theta \mathbf{R} \mathbf{T}_\theta^a\right)\Delta\mathbf{i}^\theta - \Delta\mathbf{v}^\theta$$

Control:

$$\mathbf{v}^\theta = -\overline{\varpi}\mathbf{T}_a^\theta \mathbf{\Lambda} \frac{d\mathbf{T}_\theta^a}{d\theta}\overline{\mathbf{i}}^\theta - \overline{\varpi}\mathbf{T}_a^\theta \frac{d\mathbf{T}_\theta^a}{d\theta}\boldsymbol{\lambda}_r^\theta - \mathbf{K}_P\left(\hat{\mathbf{i}}^\theta - \overline{\mathbf{i}}^\theta\right) - \int_0^t \mathbf{K}_I\left(\hat{\mathbf{i}}^\theta - \overline{\mathbf{i}}^\theta\right)dt$$

State-space:

$$\begin{bmatrix} \mathbf{T}_a^\theta \mathbf{\Lambda} \mathbf{T}_\theta^a & \mathbf{0} \\ \mathbf{0} & \mathbf{I} \end{bmatrix} \frac{d}{dt} \begin{bmatrix} \Delta\mathbf{i}^\theta \\ \int \Delta\overline{\mathbf{i}}^\theta \\ \Delta\overline{\mathbf{i}}^\theta \\ \Delta\overline{\varpi} \\ \int \Delta\hat{\mathbf{i}}_q^\theta \end{bmatrix} = \begin{bmatrix} \mathbf{A}_{11} & -\mathbf{K}_I & \mathbf{A}_{13} & \mathbf{A}_{14} & \mathbf{A}_{15} \\ \mathbf{0} & \mathbf{0} & \mathbf{I} & \mathbf{0} & \mathbf{0} \\ \mathbf{A}_{31} & \mathbf{0} & -\mathbf{A}_{31} & \mathbf{0} & \mathbf{0} \\ \mathbf{0} & \mathbf{0} & \mathbf{0} & -\omega_s & 0 \\ \mathbf{0} & \mathbf{0} & \mathbf{0} & 0 & 0 \end{bmatrix} \begin{bmatrix} \Delta\mathbf{i}^\theta \\ \int \Delta\overline{\mathbf{i}}^\theta \\ \Delta\overline{\mathbf{i}}^\theta \\ \Delta\overline{\varpi} \\ \int \Delta\hat{\mathbf{i}}_q^\theta \end{bmatrix} + \begin{bmatrix} \mathbf{B}_{11} & \mathbf{B}_{12} \\ \mathbf{0} & \mathbf{0} \\ \mathbf{0} & \mathbf{0} \\ 0 & \omega_s \\ \overline{\Omega}/E_q & 0 \end{bmatrix} \begin{bmatrix} \Delta\hat{T} \\ \Delta\omega \end{bmatrix}$$

Merz KO. Pitch actuator and generator models for wind turbine control system studies. Memo AN 15.12.35, SINTEF Energy Research, 2015.

OC3 monopile
V_∞ = 7 m/s

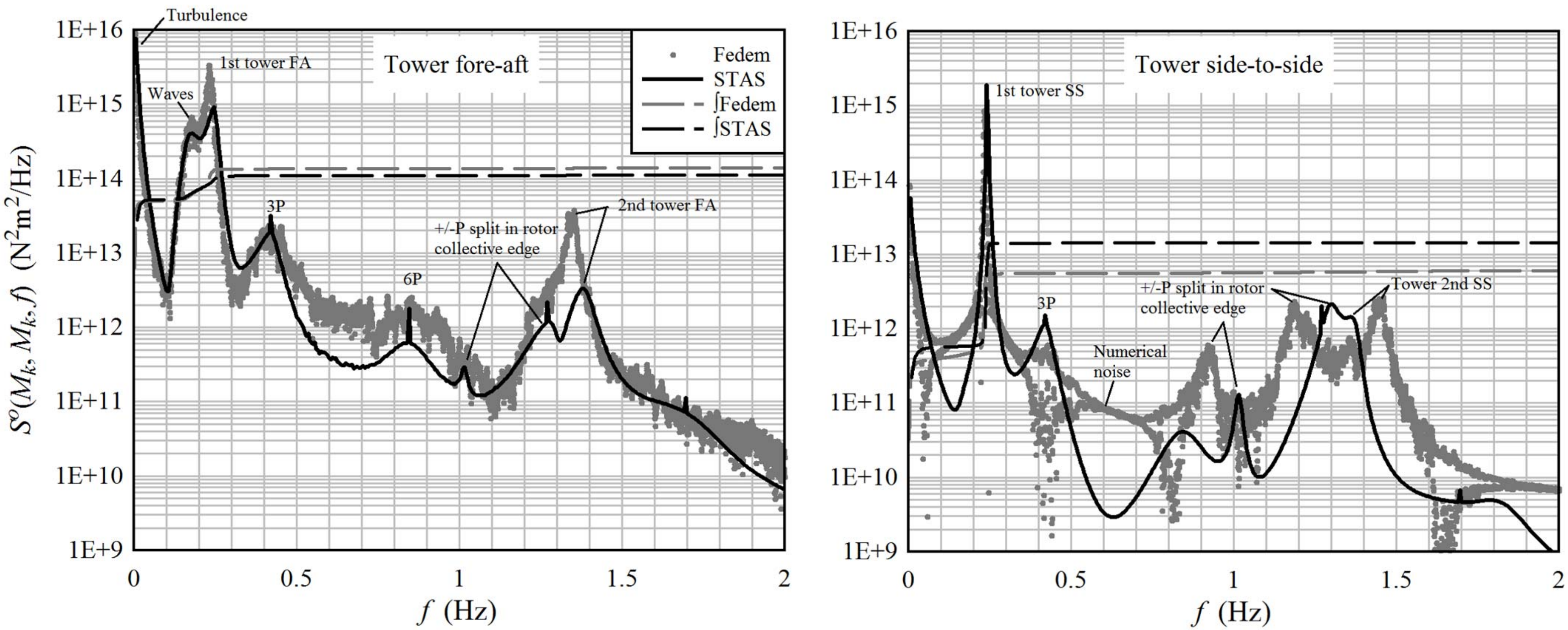

Approximate calibration to parked turbine frequencies and control gains tuned. Not a blind comparison.

$V_\infty = 11$ m/s

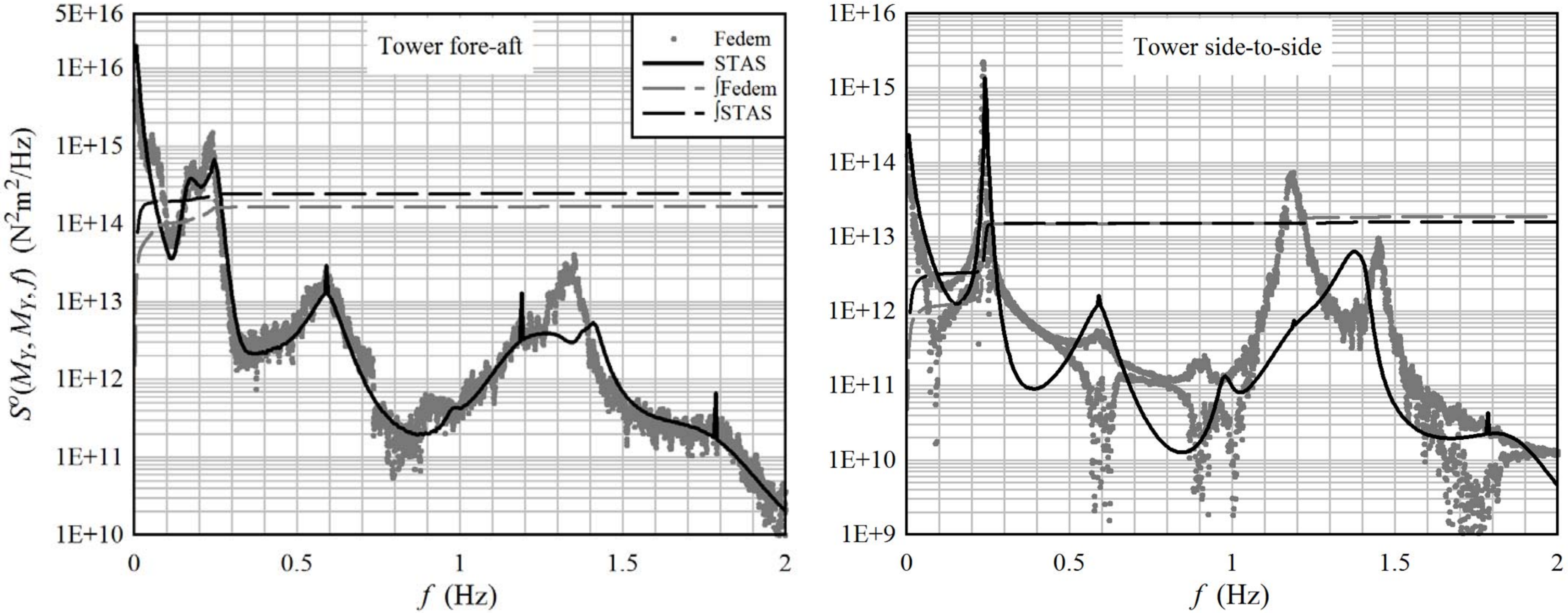
Tower fore-aft
Fedem
STAS
∫Fedem
∫STAS
Tower side-to-side
$S^o(M_Y, M_Y, f)$ (N^2m^2/Hz)
f (Hz)
5E+16
1E+16
1E+15
1E+14
1E+13
1E+12
1E+11
1E+10
1E+9
0
0.5
1
1.5
2

$V_\infty = 15$ m/s

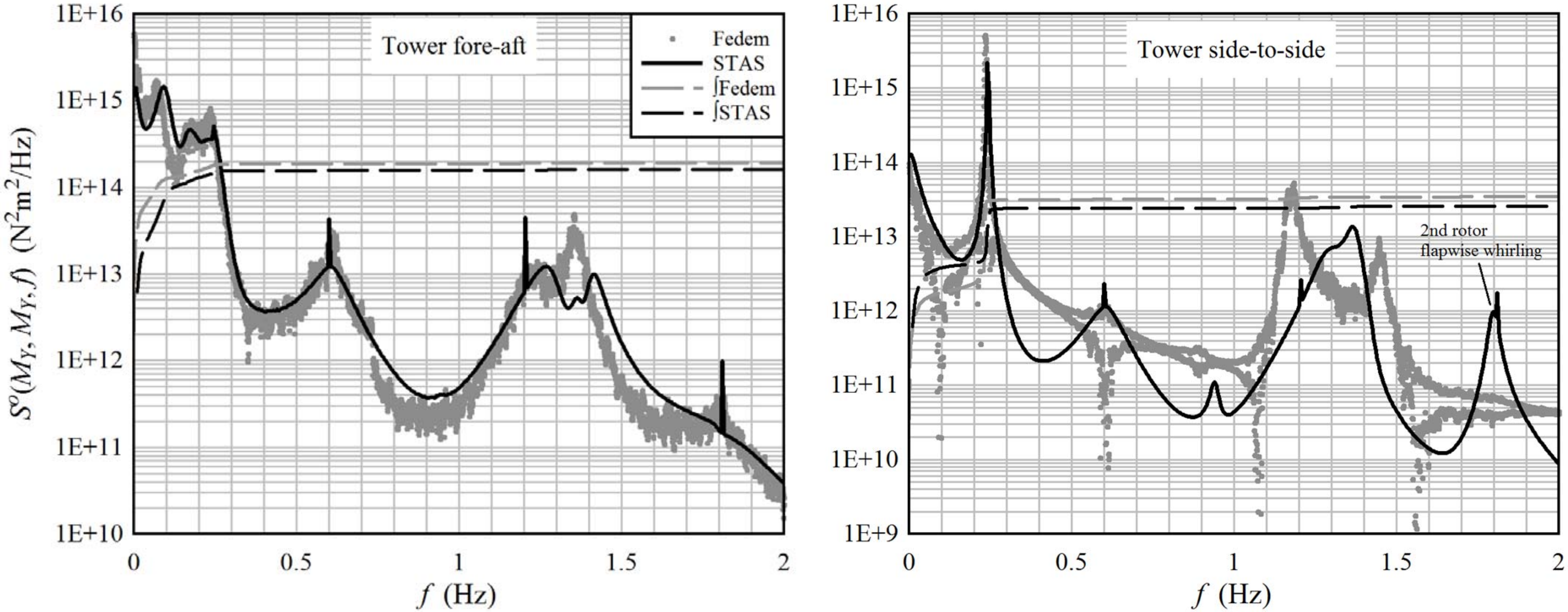
Tower fore-aft
Fedem
STAS
∫Fedem
∫STAS
$S^o(M_Y, M_Y, f)$ (N^2m^2/Hz)
1E+16
1E+15
1E+14
1E+13
1E+12
1E+11
1E+10
0
0.5
1
1.5
2
f (Hz)
Tower side-to-side
2nd rotor
flapwise whirling
1E+16
1E+15
1E+14
1E+13
1E+12
1E+11
1E+10
1E+9
0
0.5
1
1.5
2
f (Hz)

DTU 10 MW wind turbine (+ NOWITECH 10 MW nacelle), offshore foundation

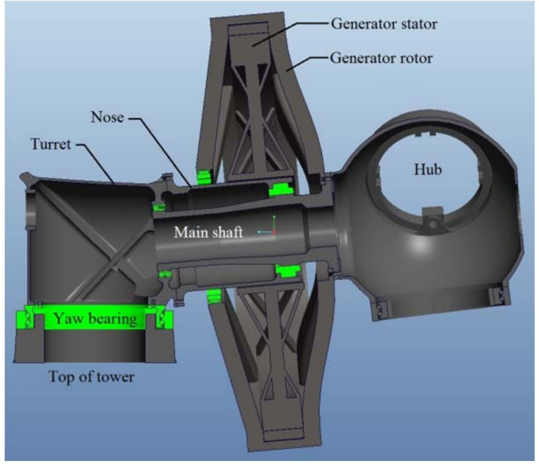

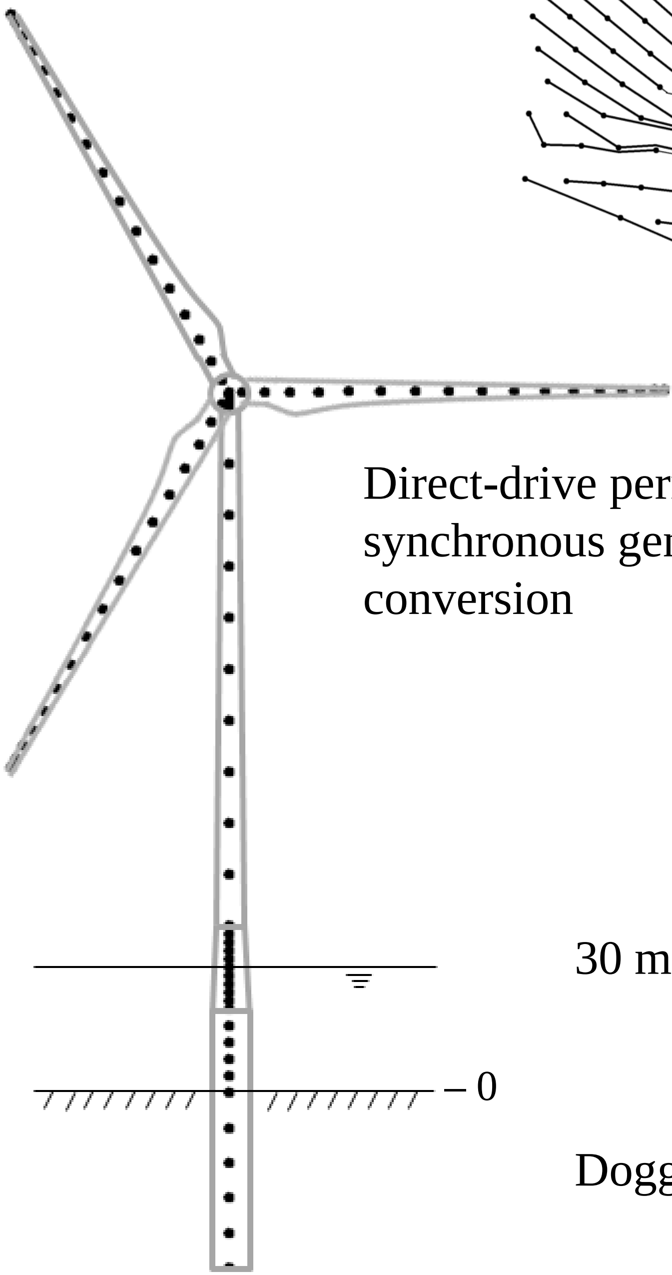

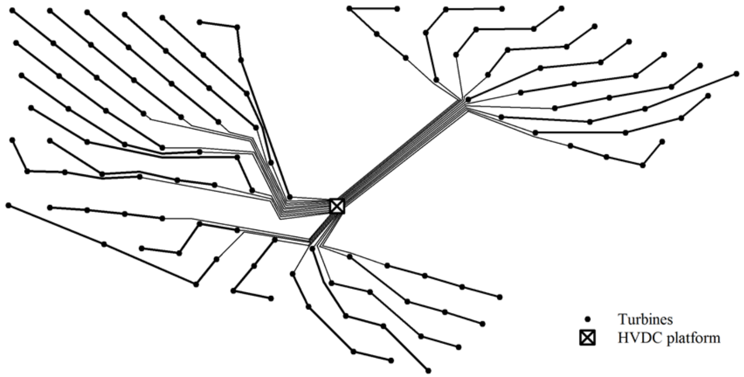

Tower +40 to +145 m
Stiffened w.r.t. onshore design
approx. 900 tonnes

Direct-drive permanent-magnet synchronous generator, full power conversion

Transition piece +20 to +40 m
approx. 600 tonnes

30 m water depth

Monopile, -42 m to +20 m
9 m diameter
approx. 1500 tonnes

Dogger Bank seabed profile

Transfer functions between waterline wave force and tower mudline bending moments

Shut down in storm

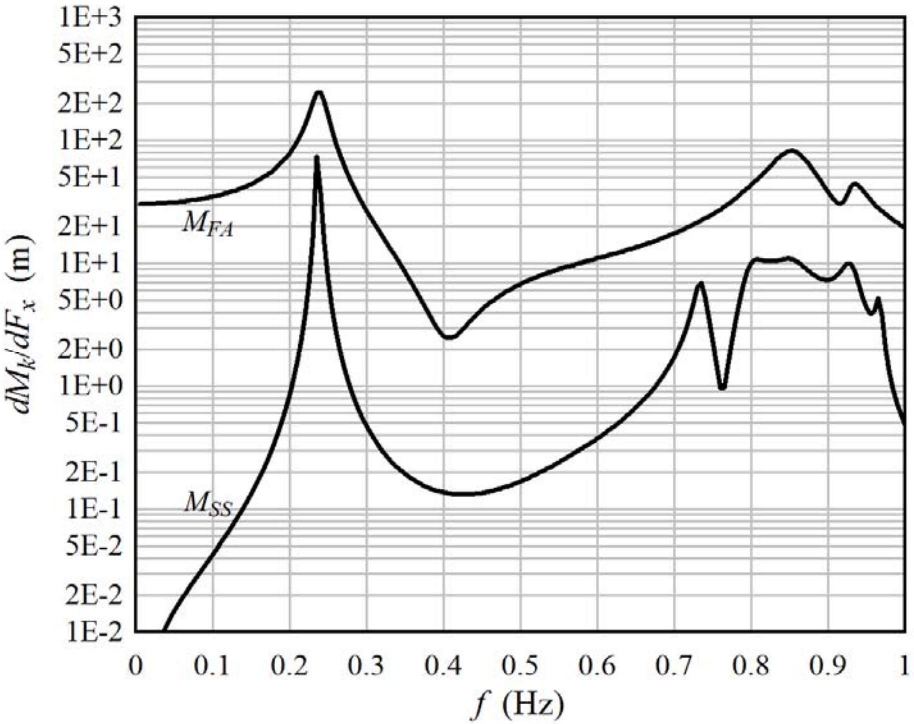

Operating at 10 m/s

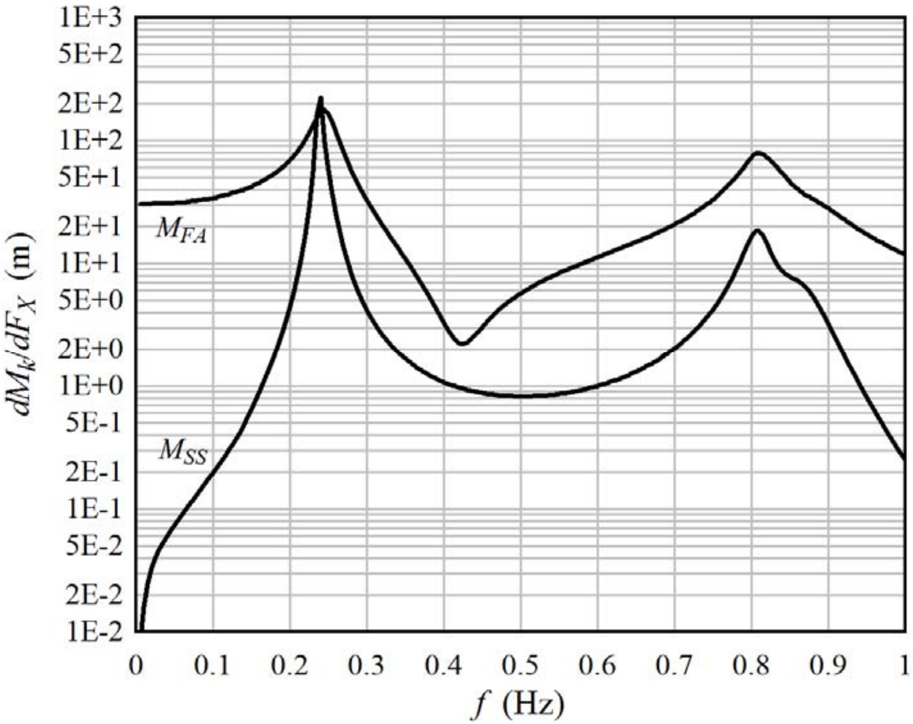

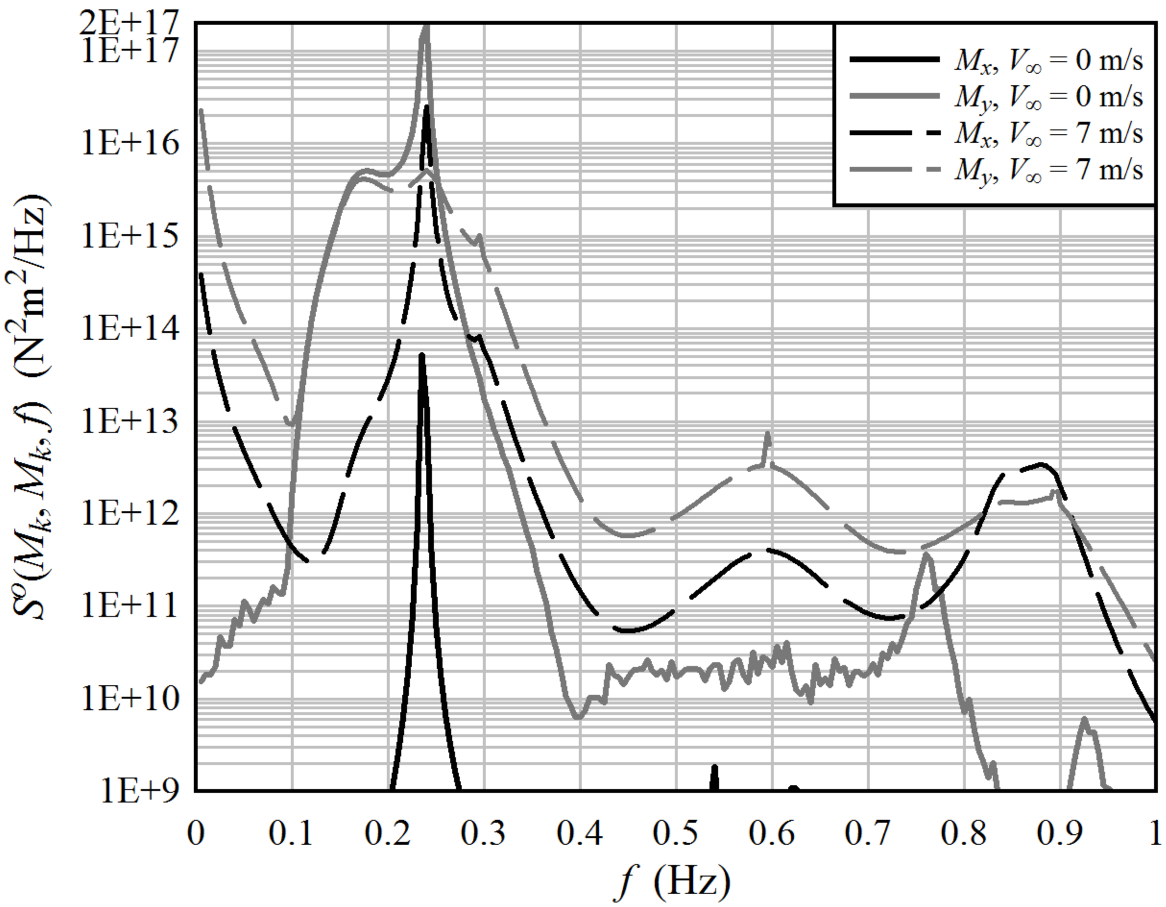

The transverse vibrations are attributed to the operating rotor.

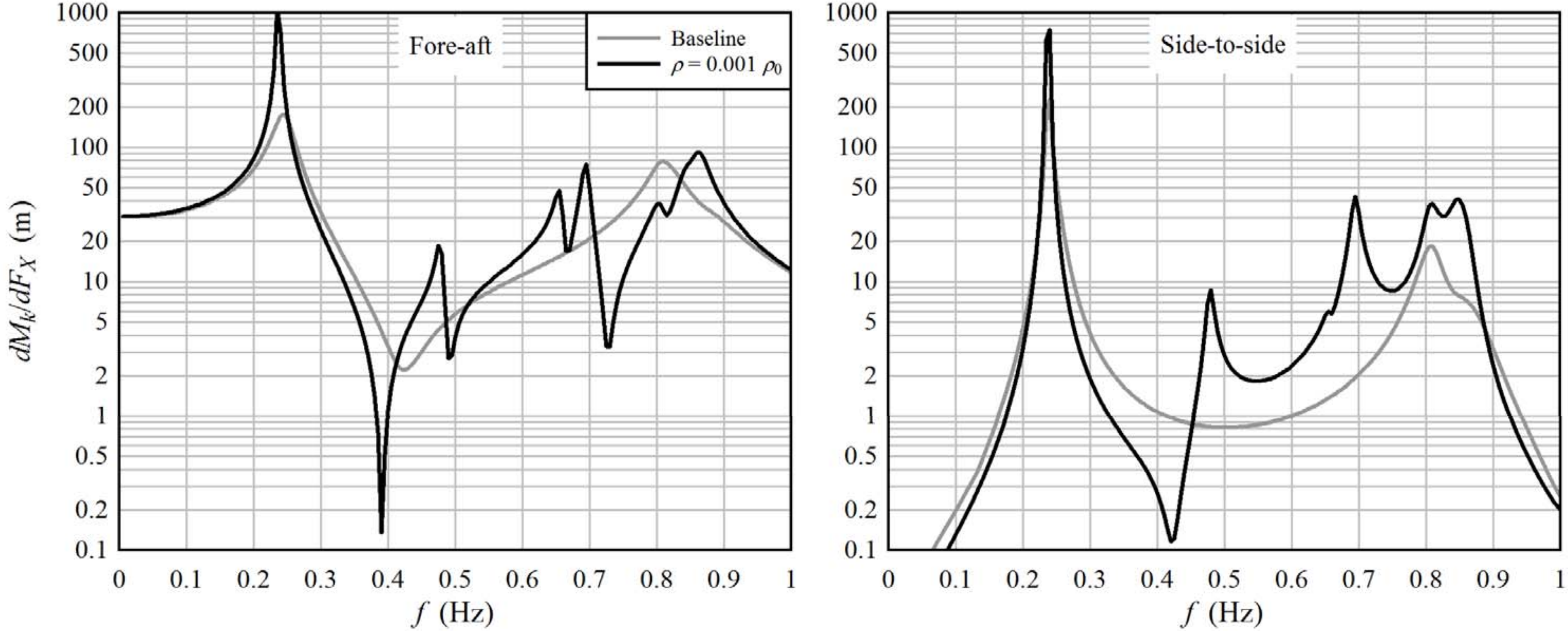

... but the interaction is nonetheless present when the rotor is spinning in a vacuum.

Hypothesis: Gyroscopic effects coupling with a rotor "nodding" component of the first tower fore-aft mode.

Load case ID	Turbine state	V_∞	θ_V	I	H_s	T_p	θ_w	V_c	θ_c
7.1-0-V	Pitch fault	1-yr	0	NTM	50-yr[1]	$E[T_p \vert H_s]$	0	1-yr	0
7.1-90-V	Pitch fault	1-yr	0	NTM	50-yr[1]	$E[T_p \vert H_s]$	90	1-yr	90
6.1-0-W	Parked	10-yr	0	NTM	50-yr	50-yr	0	1-yr	0
6.1-90-W	Parked	10-yr	0	NTM	50-yr	50-yr	90	1-yr	90
1.3-0-V	Operating	V_r	0	ETM	10-yr	$E[T_p \vert H_s]$	0	1-yr	0
1.3-90-V	Operating	V_r	0	ETM	10-yr	$E[T_p \vert H_s]$	90	1-yr	90
1.3-0-W	Operating	$\approx V_r$	0	NTM	50-yr	50-yr	0	1-yr	0
1.3-90-W	Operating	$\approx V_r$	0	NTM	50-yr	50-yr	90	1-yr	90
1.2	Operating	4...25	0[2]	NTM	$f(V_\infty)$	$f(V_\infty, H_s)$	0,45,90	$E[V_c]$	0,45,90

Environmental load probabilities

$$P\left(V_\infty, \theta_V^E, H_s, T_p, \theta_w^E\right) = P(\theta_V^E)\, P_V(V_\infty \mid \theta_V^E)\, P_H(H_s \mid V_\infty)\, P_T(T_p \mid H_s)\, P(\theta_w^E \mid \theta_V^E)$$

Table XX: Windspeed and direction bin probability.

	-180	-150	-120	-90	-60	-30	0	30	60	90	120	150
7	0.0261	0.0220	0.0268	0.0356	0.0365	0.0394	0.0403	0.0461	0.0464	0.0378	0.0311	0.0280
11	0.0113	0.0092	0.0098	0.0152	0.0192	0.0208	0.0237	0.0280	0.0276	0.0208	0.0142	0.0124
14	0.0078	0.0061	0.0054	0.0103	0.0167	0.0181	0.0239	0.0294	0.0280	0.0191	0.0103	0.0087
18	0.0027	0.0019	0.0012	0.0034	0.0094	0.0102	0.0186	0.0254	0.0224	0.0121	0.0040	0.0031

				V_∞		
		0	7	11	14	18
H_s	0	0.0260	0.0000	0.0000	0.0000	0.0000
	1	0.8600	0.8355	0.4600	0.3800	0.2000
	2	0.1095	0.1391	0.4400	0.4000	0.2500
	3	0.0042	0.0240	0.0890	0.1600	0.2600
	4	0.0003	0.0014	0.0090	0.0390	0.2000
	5	0.0000	0.0000	0.0020	0.0170	0.0600
	6	0.0000	0.0000	0.0000	0.0040	0.0211
	7	0.0000	0.0000	0.0000	0.0000	0.0081
	8	0.0000	0.0000	0.0000	0.0000	0.0008

					$T_p \mid H_s$				
		2	4	6	8	10	12	14	16
H_s	1	0.0007	0.2406	0.4658	0.2172	0.0598	0.0129	0.0026	0.0005
	2	0.0000	0.0183	0.3650	0.4203	0.1565	0.0337	0.0055	0.0007
	3	0.0000	0.0000	0.0947	0.4979	0.3221	0.0747	0.0105	0.0000
	4	0.0000	0.0000	0.0057	0.2877	0.5157	0.1709	0.0199	0.0000
	5	0.0000	0.0000	0.0000	0.0531	0.5575	0.3451	0.0442	0.0000
	6	0.0000	0.0000	0.0000	0.0000	0.2941	0.5882	0.1176	0.0000
	7	0.0000	0.0000	0.0000	0.0000	0.1000	0.6000	0.3000	0.0000
	8	0.0000	0.0000	0.0000	0.0000	0.0000	0.0000	1.0000	0.0000

							wind						
		-180	-150	-120	-90	-60	-30	0	30	60	90	120	150
waves	-180	0.2424	0.1848	0.0799	0.0196	0.0057	0.0048	0.0048	0.0048	0.0057	0.0196	0.0799	0.1848
	-150	0.1848	0.2424	0.1848	0.0799	0.0196	0.0057	0.0048	0.0048	0.0048	0.0057	0.0196	0.0799
	-120	0.0799	0.1848	0.2424	0.1848	0.0799	0.0196	0.0057	0.0048	0.0048	0.0048	0.0057	0.0196
	-90	**0.1368**	**0.1971**	**0.3020**	**0.3596**	**0.3020**	**0.1971**	**0.1368**	**0.1228**	**0.1219**	**0.1219**	**0.1219**	**0.1228**
	-60	**0.0517**	**0.0656**	**0.1260**	**0.2309**	**0.2884**	**0.2309**	**0.1260**	**0.0656**	**0.0517**	**0.0508**	**0.0508**	**0.0508**
	-30	0.0048	0.0057	0.0196	0.0799	0.1848	0.2424	0.1848	0.0799	0.0196	0.0057	0.0048	0.0048
	0	0.0048	0.0048	0.0057	0.0196	0.0799	0.1848	0.2424	0.1848	0.0799	0.0196	0.0057	0.0048
	30	0.0048	0.0048	0.0048	0.0057	0.0196	0.0799	0.1848	0.2424	0.1848	0.0799	0.0196	0.0057
	60	0.0057	0.0048	0.0048	0.0048	0.0057	0.0196	0.0799	0.1848	0.2424	0.1848	0.0799	0.0196
	90	0.0196	0.0057	0.0048	0.0048	0.0048	0.0057	0.0196	0.0799	0.1848	0.2424	0.1848	0.0799
	120	0.0799	0.0196	0.0057	0.0048	0.0048	0.0048	0.0057	0.0196	0.0799	0.1848	0.2424	0.1848
	150	0.1848	0.0799	0.0196	0.0057	0.0048	0.0048	0.0048	0.0057	0.0196	0.0799	0.1848	0.2424

All permutations:
25,920 load cases

$$S_{VM} = S_{\sigma\sigma} + 3S_{\tau\tau}$$

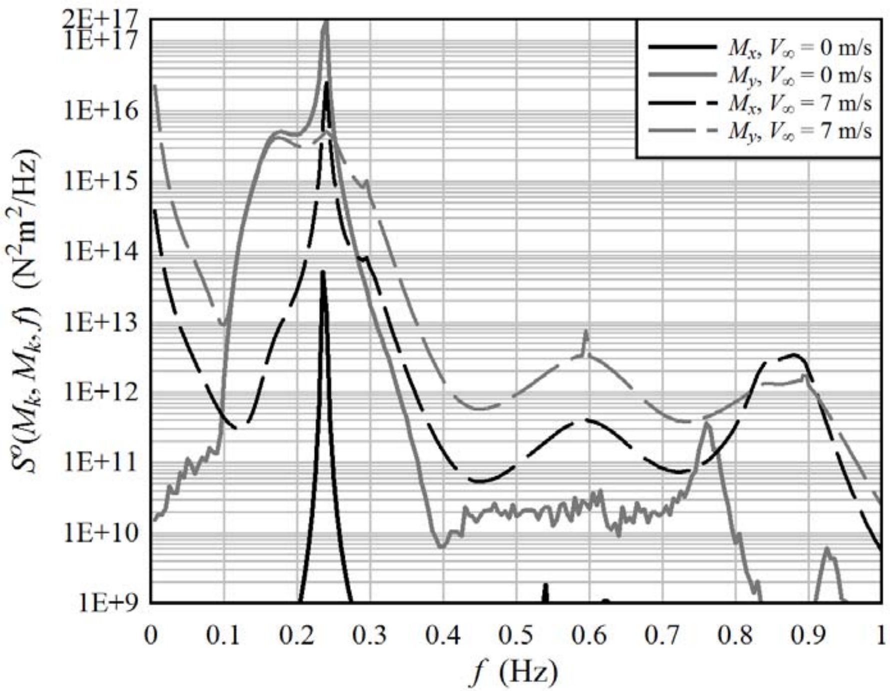

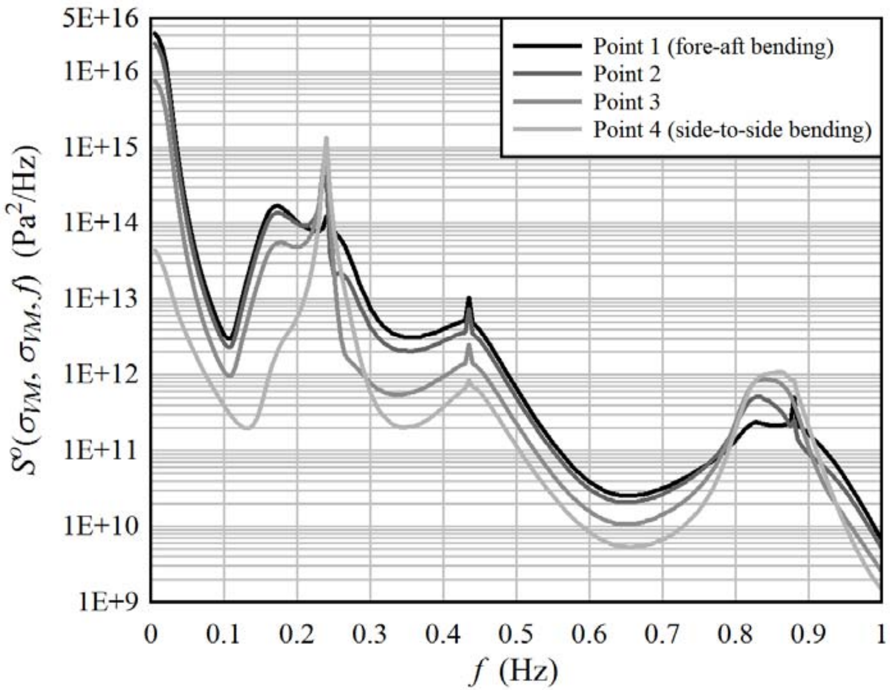

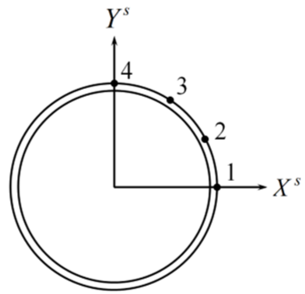

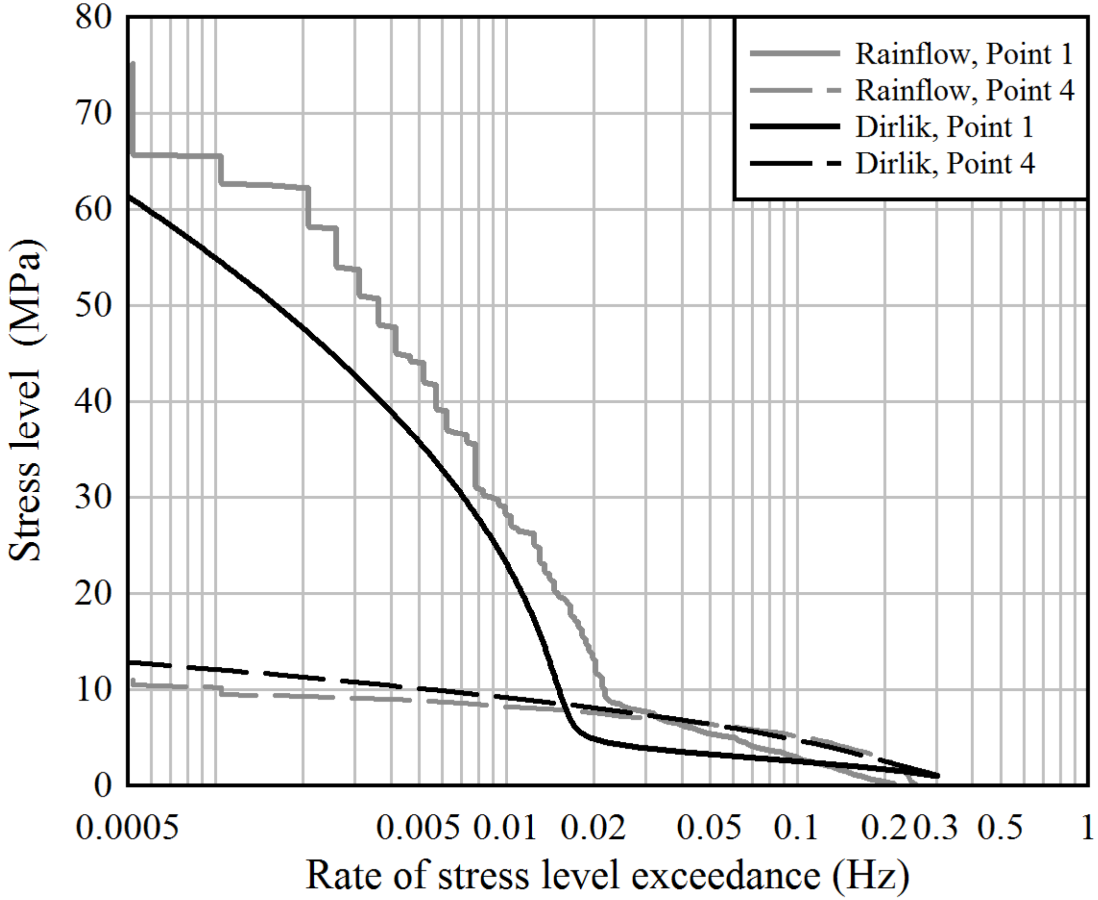

Rainflow, Point 1
Rainflow, Point 4
Dirlik, Point 1
Dirlik, Point 4
Stress level (MPa)
0
10
20
30
40
50
60
70
80
0.0005
0.005
0.01
0.02
0.05
0.1
0.2
0.3
0.5
1
Rate of stress level exceedance (Hz)

Lifetime stress cycles

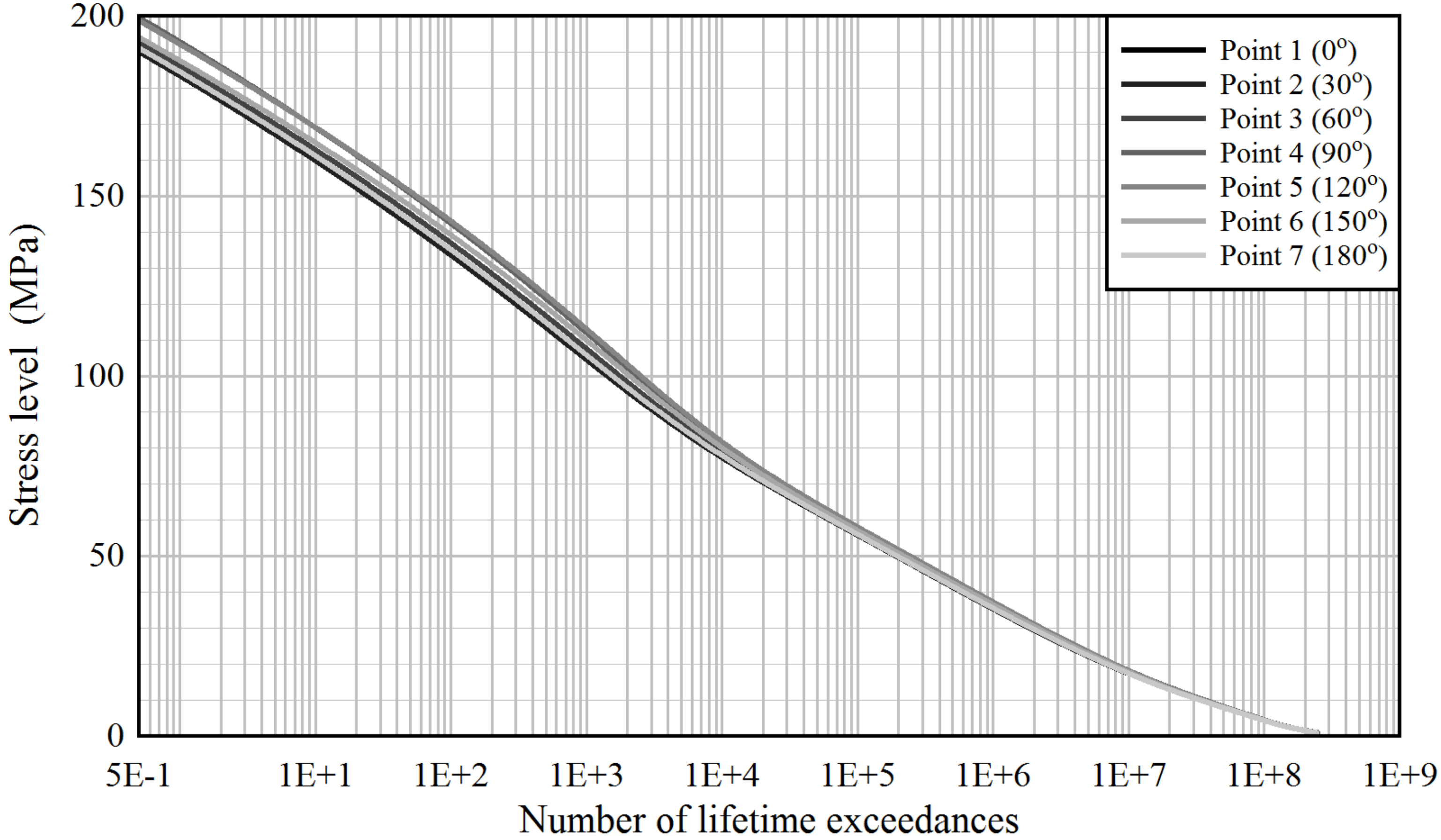

Lifetime fatigue analysis: trends with met-ocean conditions

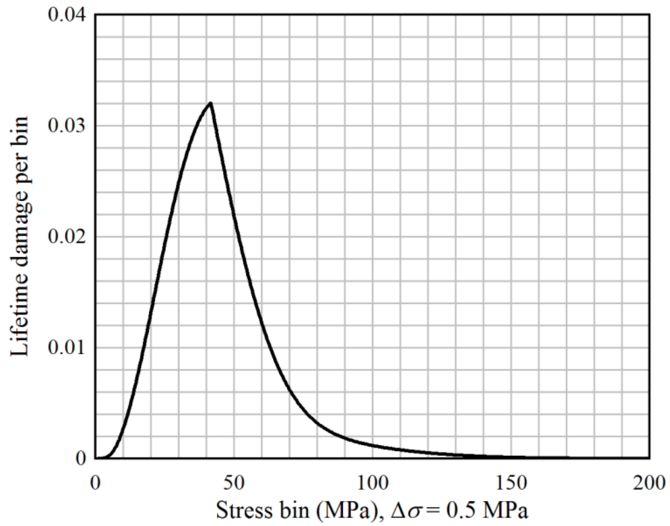

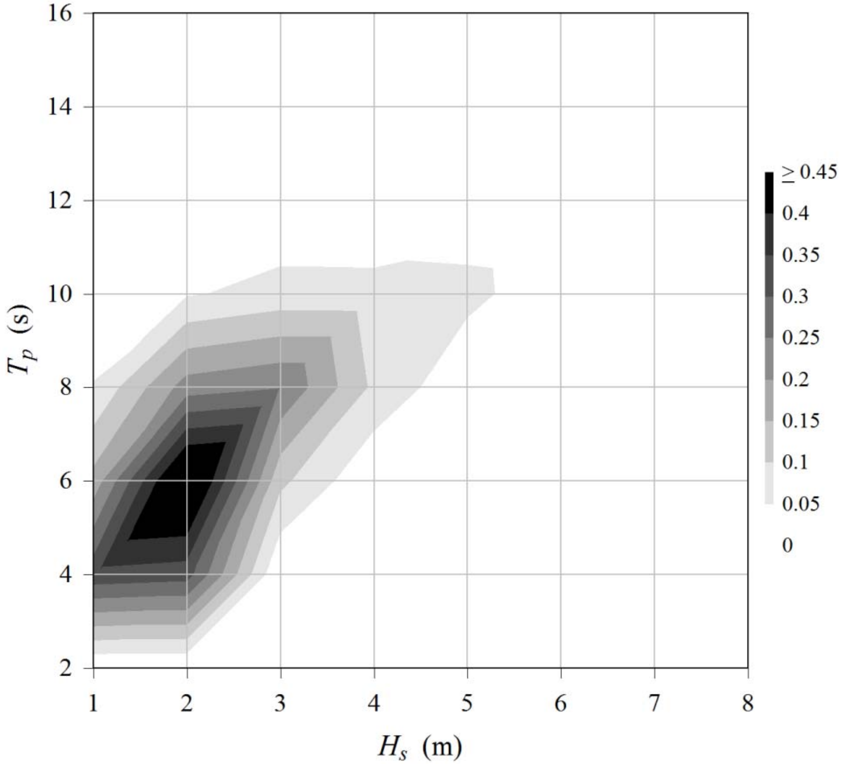

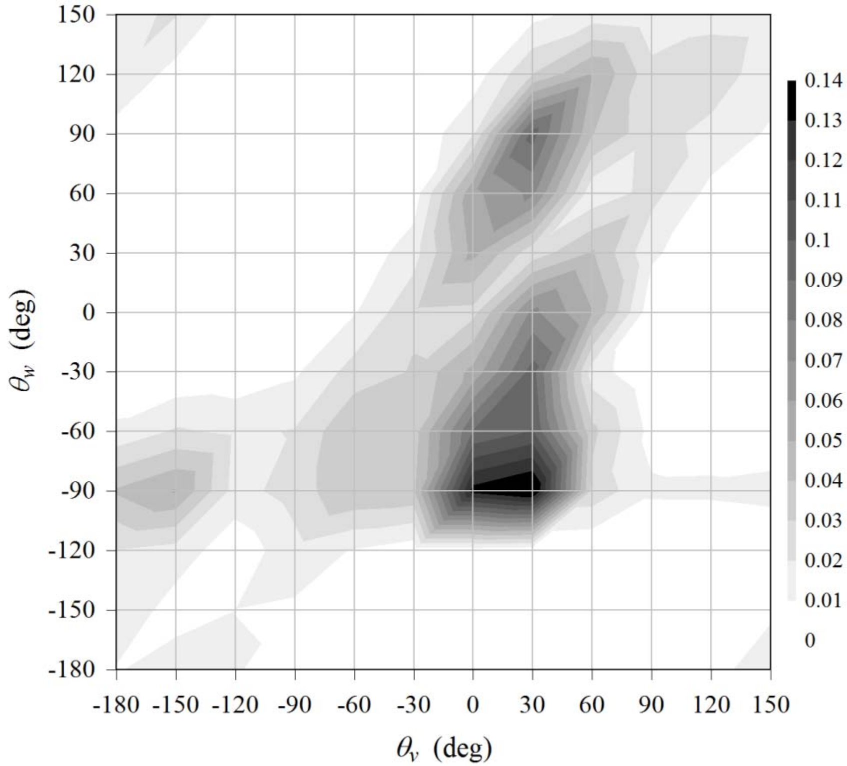

STAS program: "a wind power plant in a matrix"

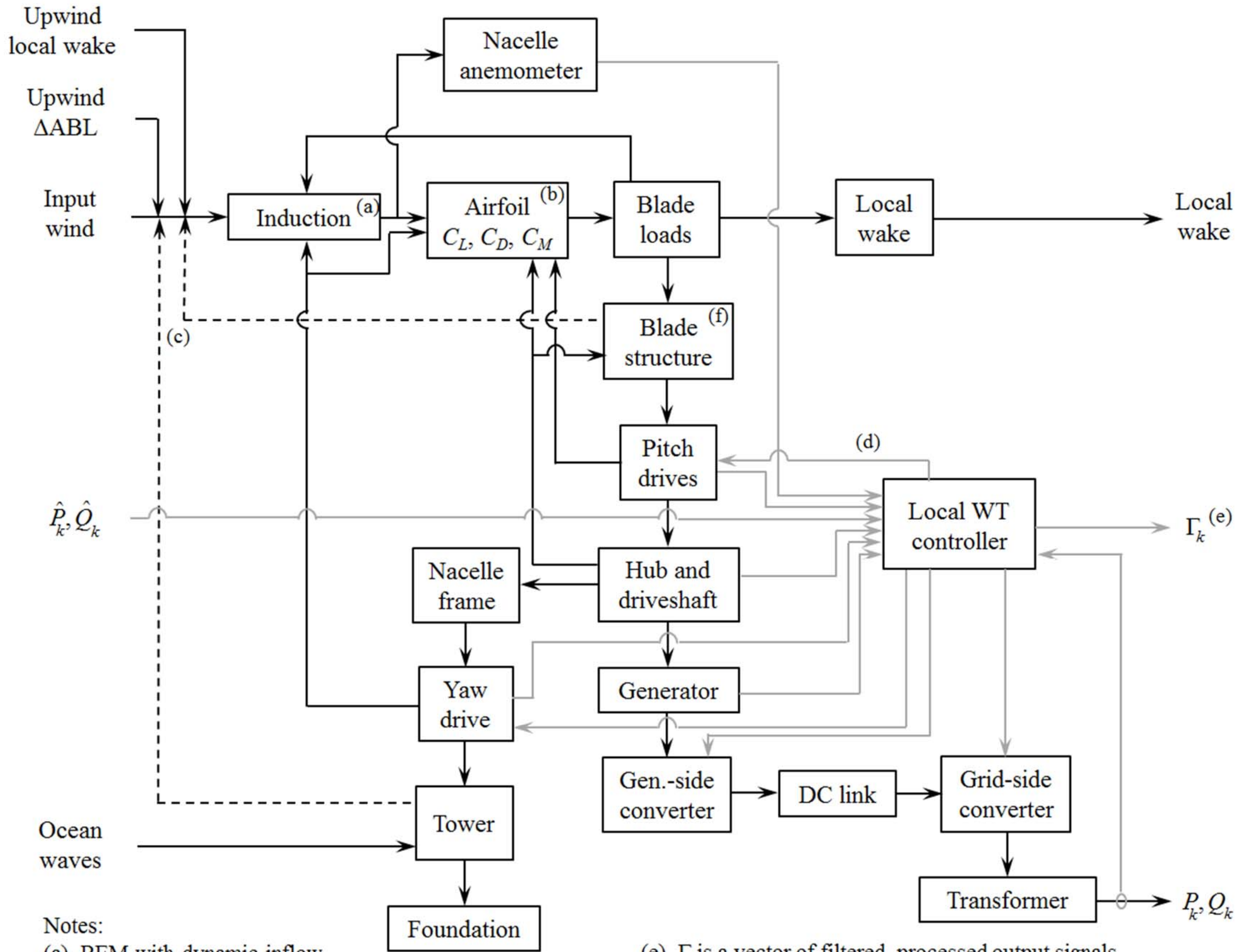

Notes:

(a) BEM with dynamic inflow

(b) Dynamic stall, Øye type model

(c) Aerodynamic damping, may be linearized and computed independently

(d) Black lines: physical connection. Grey: communication.

(e) Γ is a vector of filtered, processed output signals.

(f) Additional load, strain, or acceleration sensors could be installed in any of the mechanical components and fed to the local controller for active damping or inclusion in the output signal vector Γ.

STAS program: "a wind power plant in a matrix"

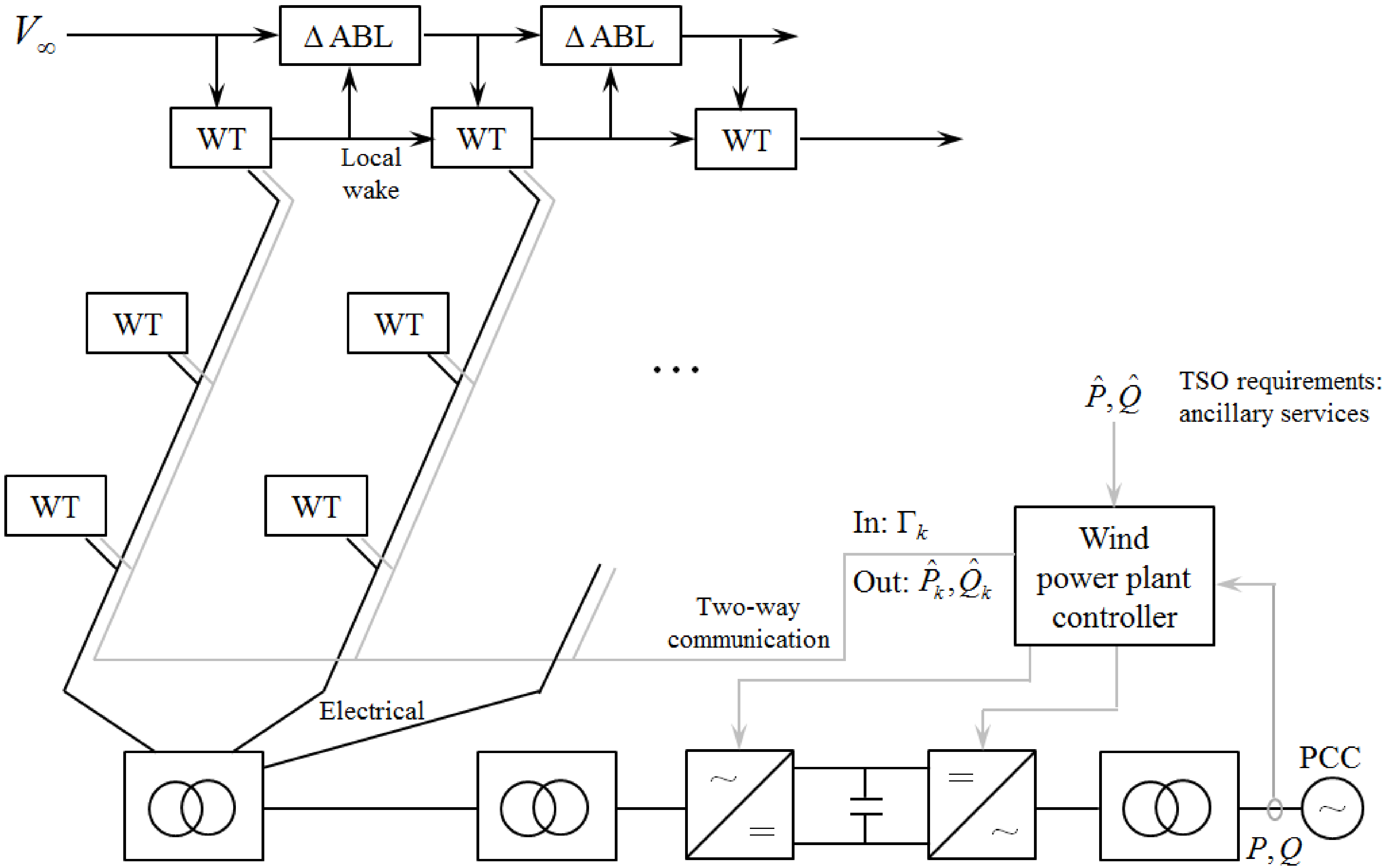

(End of presentation.)